THE NATURE OF MARE BASALTS IN THE PROCELLARUM KREEP TERRANE. Larry A. Haskin, Jeffrey J. Gillis, Randy L. Korotev, and Bradley L. Jolliff, Department of Earth and Planetary Sciences and McDonnell Center for the Space Sciences, Washington University, One Brookings Drive, St. Louis, MO 63130 (lah@levee.wustl.edu)

Introduction: The most common morphologic feature of the Procellarum KREEP Terrane (PKT) is volcanic plains. Here, we use chemical information from sample studies, Lunar Prospector Th concentrations (2° pixels; [1]), Clementine FeO and TiO_2 concentrations [2] (convolved to 2° resolution), and geologic mapping to determine some characteristics of basalt types of these plains. We might have expected that most of the mare basalts would be low in Th concentrations, like nearly all mare basalts sampled by the Apollo 12 and 15 missions (~0.5–1 ppm; [4]). Instead, we show here [see also 3] that most basalts of the PKT have higher Th concentrations (typically, 2.5–6 ppm, some probably higher) and a broad range of TiO_2 concentrations (<1% to ~15%; [see also 5, 6]). Such basalts have not been identified in the lunar sample collection, but some glasses sampled within the PKT have similar characteristics.

The PKT as defined here is the area of the Imbrium-Procellarum region within a contour drawn at 3 ppm Th, based on results of Lunar Prospector [1] (Fig. 1). We have classified each of the 2° pixels of Lunar Prospector within the PKT as mare, terra (i.e., nonmare, such as Alpes or Fra Mauro formations), or "mixed" strictly on the basis of geologic maps [7]. Then, we examined the trends of chemical composition of the materials sensed remotely according to pixel type. For a pixel to qualify as terra or mare, the area underneath it had to be mapped as ≥90% one or the other; all other pixels are "mixed." Some 18% of the pixels cover terrae, 38% mare, and 43% mixed

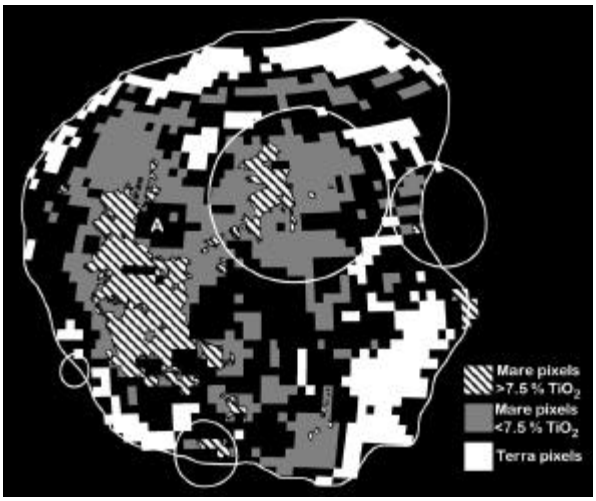

Figure 1. Pixel map of the Procellarum KREEP Terrane. Black areas within the boundary are the "mixed" pixels. Mare pixels have been subdivided by their TiO_2 composition. Circles in order of decreasing size represent the Imbrium, Serenitatis, Humorum, and Grimaldi basins. A is the location of the Aristarchus Plateau. The map is an equal-area Lambert projection centered on 30° W and the equator.

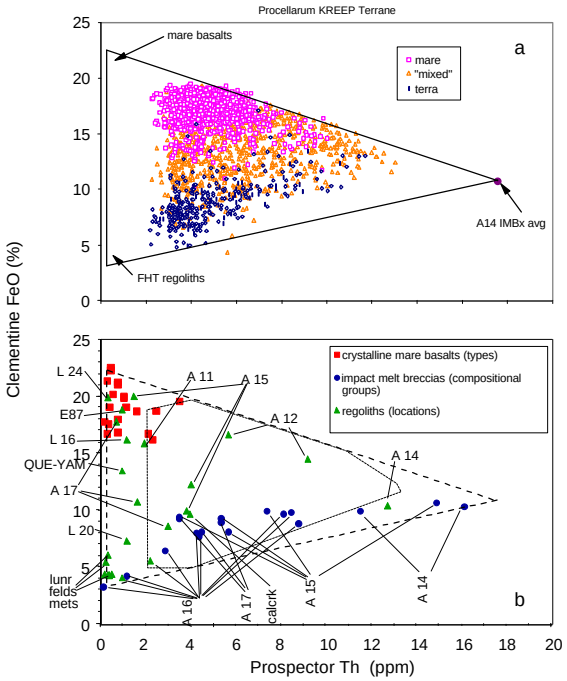

Figure 2. (a) Th and FeO for terra, mare, and mixed pixels of the PKT (data from [1,2]). **(b)** Average Th and FeO for lunar samples: mare basalts, regoliths, and mafic impact-melt breccias [4].

(Fig. 1). The term "mixed" means that a boundary between mare and terra occurs within the pixel. A pixel mapped as mare, terra, or mixed may have a regolith containing both mare and terra materials.

Discussion: *Remote sensing data and sample data:* Pixels classified as mare cluster in the range 3–7 ppm Th (some higher) and 15–20% FeO (Fig. 2a). The high FeO concentrations (mostly >15%) of the mare pixels indicate that at the pixel scale the lavas are mare basalt (samples typically ≥20% FeO, but as low as ~16%) not KREEP basalt (~10% FeO).

Terra pixels plot along the lower (i.e., low-FeO) boundary of the point distribution. The range begins at relatively low FeO (~5%) and Th (~2 ppm) and extends toward the composition of the Apollo 14 soil (the highest-Th mixed-pixel point). The pixel data fit well inside a triangle whose apices correspond to samples: (1) regolith of the Feldspathic Highlands Terrane, as represented by the feldspathic lunar meteorites, (2) mare basalts, and (3) "KREEP," as represented by impact-melt breccias from Apollo 14 ("A14 IMBx," Fig. 2a). Figure 2b compares average Th and FeO concentrations of other materials from the lunar sample collection (summarized by [4]) with the distribution of Lunar Prospector and Clementine data. The most common type of crystalline polymict rock in the

Apollo collection, the mafic impact-melt breccias, plot along the lower edge of the pixel data (Fig. 2). Based on Figure 2 alone, we might conclude that all major types of material present within the PKT are well represented in the lunar sample collections. This is not entirely allowed by the FeO-TiO_2 distribution, however.

Mare Basalt composition: Figure 3 requires that regoliths represented by most mare pixels be composed predominantly of basalts. Also, the mare basalts a wide range of TiO_2 concentrations. Mixing of low-TiO_2 basalt with the more common Th-rich materials found in the sample collection, or even with the more rare ones (KREEP basalt, granite-felsite, quartz monzodiorite), cannot simultaneously satisfy the FeO, TiO_2, and Th concentrations and their interrelationships as seen in the mare pixels. Pixels having FeO concentrations ≥18% and >7.5 % TiO_2 determine the high-FeO apex of the data triangle in Figure 2a. The location (southwestern Procellarum) and age (Eratosthenian) of these basalts has minimized their contamination by nonmare materials. Most are distant from terra regions (Figure 1) and few impact craters have excavated terra from beneath them. Thus, as seen in Figure 3, mixed pixels between high-Ti basalt and Th-rich terra materials are rare.

Figure 3 shows a continuous distribution of mare pixel compositions that starts at FeO ~19% and TiO_2 ~15% and leads steeply downward to FeO ~15–16% and TiO_2 ~2–3%. This indicates the presence of basalts with essentially the same range of TiO_2 concentrations. The substantial presence of high-Ti basalts in the Procellarum KREEP Terrane was indicated earlier from ground-based remote-sensing studies using VIS-NIR reflectance spectroscopy, [e.g., 5,8,9]. We compare this distribution to that for lunar volcanic glasses collected within and near the PKT (the "picritic" glasses, [10, 11], Fig. 3). These glasses have a similar distribution of TiO_2 concentrations. The mare pixels (Fig. 3) are systematically offset to lower FeO concentrations relative to the volcanic glasses. Some offset is expected because the volcanic glasses have more mafic bulk compositions than mare basalts. Some offset, especially for lower-TiO_2 basalts, may result from mixing with lower-FeO, non-mare materials.

The volcanic glasses are not mare basalts, but their compositions indicate the variability and nature of the deep mantle beneath the Procellarum KREEP Terrane. Most have KREEP-like relative rare-earth abundances from which we can estimate their Th concentrations [e.g., 12]; they range from ~2 to ~5 ppm. Dark mantling deposits of pyroclastic glass are not widespread or abundant enough in the PKT to account in general for the high Th and TiO_2 concentrations of the mare pixels. Two samples of high-Th impact glasses may come from PKT basalts: an Apollo 15 yellow impact glass clod (15010,3189) with ~8 ppm Th, 19% FeO, and 4.2% TiO_2 [13] and an Apollo 14 glass bead (14161,7127) with 5.4 ppm Th, 20% FeO, and 4.4% TiO_2 [14]. Apollo 14 aluminous and very-high-K basalts have Th concentrations approaching 3 ppm [15-17].

Most PKT basalts have >2 to ~6 ppm Th, some perhaps higher (Fig. 2a). The highest-Th (>5 ppm) mare pixels occur in groups. These groups are not in general coincident with the TiO_2-rich basalts shown in Figure 1.

Figure 3. FeO and TiO_2 for terra, mare, and mixed pixels, with ranges indicating the principal corresponding sample materials. The population of mixed pixels is more dense than shown, especially up to ~6% TiO_2, being overlain with mare pixels in this diagram.

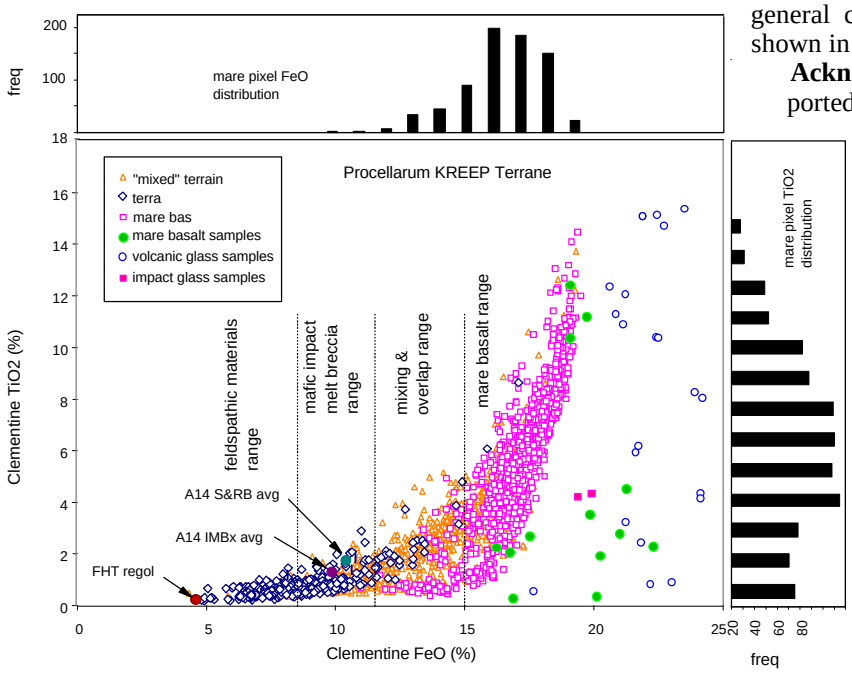

Acknowledgements: This work was supported by NASA under grants NAG5-4172, NAG5-8609, and NAG 5-6784.

References: [1] Lawrence et al.(1999) *GRL* **26**, 2681–2684; [2] Lucey et al. (in press) *JGR*; [3] Jolliff et al. (in press) *JGR*; [4] Korotev (1998) *JGR* **103**, 1691–1701; [5] Pieters (1978) *PLPSC 9*, 2825–2849; [6] Giguere et al. (1999) *LPSXXX*, #1465; [7] Wilhelms & McCauley (1971) USGS Map I-703; [8] Pieters et al. (1980) *JGR* **85**, 3913–3938; [9] Gillis et al. (this volume); [10] Shearer and Papike (1993) *GCA* **57**, 4785-4812; [11] Papike et al. (1998) *Revs. Mineral.* **36**, 5-1 to 5-234; [12] Haskin and Warren (1992) *Lunar Sourcebook*, 357–474; [13] Delano et al. (1982) *PLPSC 13*, A159–A170; [14] Jolliff et al. (1991) *PLPSC 21*, 193–219; [15] Dickinson et al. (1985) *PLPSC 15*, C365–C374; [16] Shervais et al. (1985) *PLPSC 15*, C374–C395; [17] Shervais et al. (1986) *PLPSC 16*, D3–D5.